

Development of a smart portable cupping suction device with multi-mode control using PID regulation

Mohd Riduwan Ghazali, Mohd Ashraf Ahmad, Luqman Hakim Akmalmas

Faculty of Electrical and Electronic Engineering Technology, Universiti Malaysia Pahang Al-Sultan Abdullah, Pekan Pahang, Malaysia

Article Info

Article history:

Received Apr 30, 2025

Revised Jul 7, 2025

Accepted Jul 12, 2025

Keywords:

Differential pressure sensor
Multi-mode suction
PID control
Portable cupping device
Real-time pressure regulation

ABSTRACT

Cupping therapy is a well-established traditional treatment with various health benefits. However, existing electric cupping devices lack precise pressure control and portability which limit their usability across different skin types. This paper presents the development of a smart and portable cupping suction device with multi-mode functionality for dry, wet, and massage cuppings. Designed using an ESP32C3 XIAO microcontroller, a differential pressure sensor (MPX5100DP), and a motor driver (L293D) to enable real-time pressure regulation, the system incorporates a proportional-integral-derivative (PID) to maintain a consistent suction performance at the negative pressures of -25, -35, and -45 kPa. The device was tested on different skin conditions of clean, less hairy, and slightly hairy surfaces. A real-time monitoring interface was additionally integrated using a web server to track the variation in pressure. Experimental results demonstrate effectiveness of the PID control system in achieving stable pressure with minimal fluctuations with enhanced user safety and comfort. It advances the medical devices for therapeutic automation by offering a portable, precise, and user-friendly cupping solution.

This is an open access article under the [CC BY-SA](#) license.



Corresponding Author:

Mohd Ashraf Ahmad

Faculty of Electrical and Electronic Engineering Technology, Universiti Malaysia Pahang Al-Sultan Abdullah
26600 Pekan Pahang, Malaysia

Email: mashraf@umpsa.edu.my

1. INTRODUCTION

Known as “hijama” in Arab, cupping therapy is a widely practiced traditional therapeutic technique that has been promoting health and treating various ailments through centuries [1], [2]. The process creates suction on the skin for enhanced blood circulation which boosts immunity and facilitates detoxification [3], [4]. It is further classified into dry cupping which solely relies on suction to relieve pain and promote relaxation, and wet cupping which controls incision to induce bloodletting for therapeutic benefits [5], [6]. Alternatively, moving cupping prevails as a cupping technique that continuously glides cups over lubricated skin to offer the effect of dynamic massage for enhanced therapeutic impact [7], [8]. The integration of moving cupping therapy and acupoint bloodletting is further empirically validated to effectively alleviate the symptoms associated with skin lesions [9], [10].

The suction mechanism in cupping therapy operates through the reduction of air pressure inside the cup to draw the enclosed skin and underlying tissues upward, while expanding the capillaries [11]. The application of negative pressure to the skin conforms Taibah’s theory for reduced capillary pressure to facilitate increased blood flow and detoxification [12]. Modernization of this therapeutic approach is accordingly observed on the transition of using cups as tools for timed suctions in traditional cupping, to the employment of

rubber pumps or silicone cups for improved convenience and control [13], [14].

Even so, effectiveness of cupping therapy is immensely affected by the variability in surface of the skin. Hairy skin especially requires higher suction pressure to maintain adhesion due to its tendency to disrupt the vacuum seal [1]. Similarly, areas with higher sensitivity such as the face necessitates the use of a lower pressure to prevent bruising and discomfort [15], [16]. Addressing these variations saw the introductions of multi-mode cupping devices which allow adjustable suction intensity based on the targeted area. Correspondingly classified three different levels of suction intensities in cupping therapy: light cupping (-100 to -300 mbar or -10 to -30 kPa) which is suitable for children, older individuals, and facial treatments with a higher proneness to cup detachment [17], medium cupping (-300 to -500 mbar or -30 to -50 kPa) which is effective for the relieving of muscle pain relief and improving blood circulation with a high possibility of leaving temporary marks [18], and strong cupping (≤ -500 mbar or -50 kPa and above) which is used for deep tissue therapy with lesser suitability for sensitive skin areas from its risk of irritation and discomfort [19].

Continuous advancement in cupping technology has continuously uncovered numerous limitations amidst current implementation. Manual cupping tools with piston-handle pumps and valve cups are commendable on their adjustable suction intensities from the number of pulled handles [20], [21]. Nevertheless, mechanical wear can result faulty valves that cause unreliable vacuum retention. Electric vacuum cupping devices instead provide stronger suction at a maximum pressure of -600 mmHg (-73.32 kPa) [22]. The enhanced therapeutic effectiveness comes with the cost of integrated pressure sensors for precise real-time monitoring of the cupping process, where existing risk of overpressure can lead to skin irritation and blister. Moreover, majority of these devices demand a main source of power that restricts portability and limits usability in diverse settings [23].

In address the mentioned challenges, this research proposes and develops a smart and portable cupping suction device as powered by a rechargeable battery by the integration of multi-mode functionality and a differential pressure sensor to enable both precision and consistency in suction control. A proportional-integral-derivative (PID) control [24], [25] system has been implemented to regulate the negative pressure across the different skin conditions of hairy, clear, and facial surfaces for practical adaptability and effectiveness. By incorporating real-time pressure monitoring via a web interface, the proposed system is aimed to enhance the safety and usability, with improved therapeutic outcome [26], [27].

2. METHOD

The development process commenced with a comprehensive review of system requirements on both aspects of hardware and software specifications. Following this, the project proceeded through the linearly organized stages of hardware design, circuit development, software implementation, and system validation. Hardware fabrication involves the design and production of device enclosures with aid from the 3D printing technology. Circuit development includes schematic design and printed circuit board (PCB) layout generation for key electronic components. Upon the completing software programming, system performance was rigorously tested. Iterative refinements were further applied to achieve optimal functionality and reliability.

2.1. Hardware design

3D design of the portable cupping suction device, as shown in Figure 1, features the upper and lower sections in a compact two-compartment architecture with two auxiliary mounts incorporated to secure the motor and cupping head. The top compartment houses the PCB, OLED display, and a charging module which is accessible via purpose-built openings. The lower compartment accommodates the battery and motor pump which are secured within a robust enclosure. Both compartments are connected using buckle locks for superior mechanical stability. Furthermore, cup used for cupping is affixed beneath the bottom casing, with a stop switch being positioned laterally and directly wired to the battery's positive terminal for straightforward power control.

PLA+ material was selectively used to fabricate the enclosure, owing to its enhanced mechanical properties over conventional PLA. Offering superior durability, flexibility, and printability, PLA+ is well-suited to endure mechanical stress as exerted by the motor throughout the prolonged operation. An exploded view of the device's components and their assembly process is depicted in Figure 2.

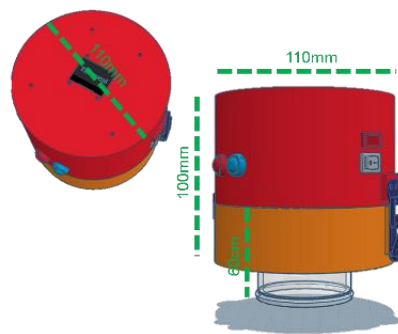


Figure 1. 3D model of the portable cupping suction device

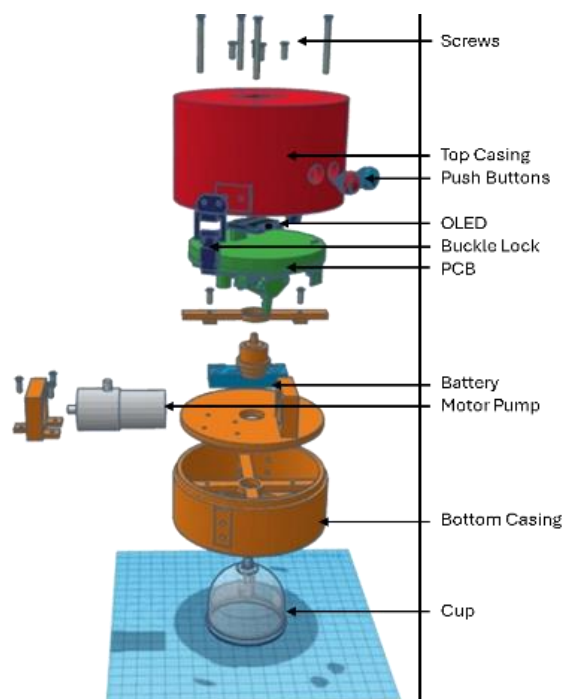


Figure 2. Exploded view of the portable cupping suction device

2.2. Circuit design

This section presents the overall system architecture, the detailed electronic schematic, and the finalized PCB layout. Electronic design of the portable cupping suction device especially integrates critical components to achieve reliable control, precise suction regulation, and compact system implementation. The system architecture, as illustrated in Figure 3, comprises the three main modules of user interface, control circuitry, and actuation mechanisms. User inputs are managed through the tactile push buttons, while having the system status and real-time pressure readings being displayed on a compact OLED screen. Observably, a differential pressure sensor (MPX5100DP) provides continuous feedback to enable a closed-loop pressure regulation.

The power is supplied by a 7.4 V lithium polymer (LiPo) battery. Motor operation sees a 12 V voltage elevation using a buck-boost converter, with microcontroller (ESP32C3) and auxiliary peripherals see the stepping down of voltage to 5 V using a 7805 linear voltage regulator. Motor actuation is controlled by an L293D motor driver by receiving pulse-width modulation (PWM) signals from the microcontroller. Additionally, safe and convenient battery maintenance is supported by an integrated battery charging module without the need for circuit disassembly.

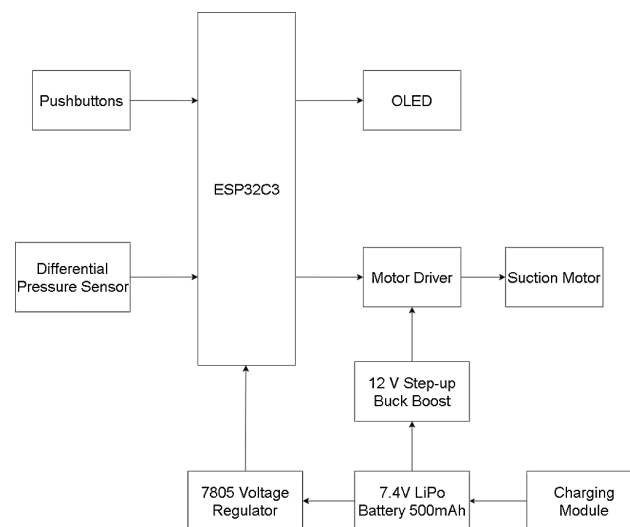


Figure 3. System block diagram of the portable cupping suction device

The complete circuit schematic is shown in Figure 4. A 12 V motor pump is connected to the L293D driver, which interfaces directly with the ESP32C3 microcontroller for precise motor speed and direction control. Besides, the MPX5100DP pressure sensor outputs an analog signal proportional to suction pressure as captured and registered by analog input (A0) of the microcontroller.

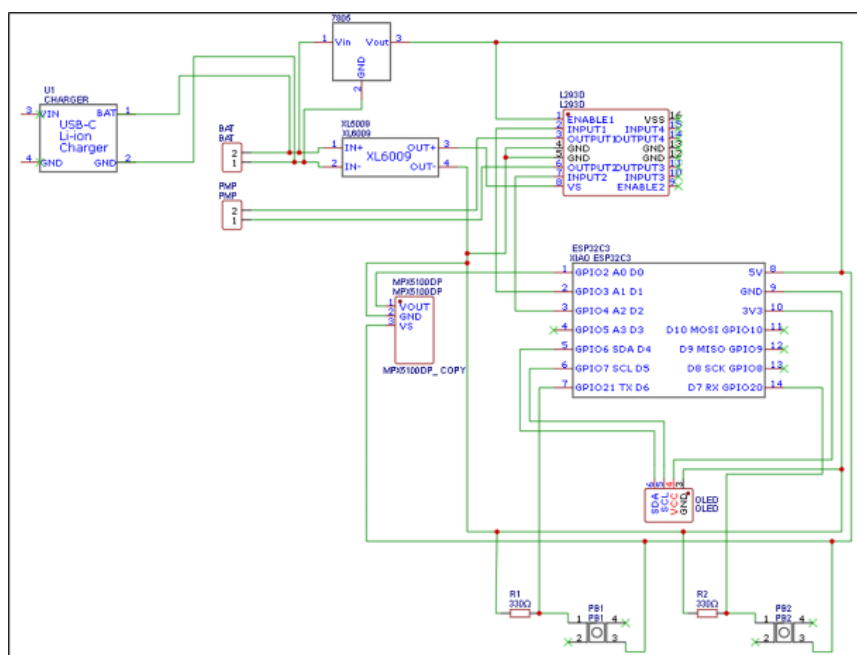


Figure 4. Schematic diagram of the electronic circuit

The user interface consists of two push buttons as configured for mode selection and suction activation. In this case, pull-down resistors are employed to stabilize the input signals and prevent floating states. The OLED display is connected via general-purpose I/O (GPIO) pins (D4 and D5), with the motor control signals

being routed through D1 and D2. The power management circuit enables seamless transition between device operation and battery charging which protects the device against conditions of overvoltage and overcurrent during the charging process.

The finalized PCB layout, as depicted in Figure 5, was optimized for minimal form factor, while ensuring signal integrity and effective thermal management. Strategic placements of high-current paths, sensitive analog signals, and ground planes were implemented to reduce electromagnetic interference for improved overall robustness. Key components, including ESP32C3, MPX5100DP pressure sensor, power converters, and user interface elements, were efficiently arranged for balanced accessibility, manufacturability, and mechanical stability.

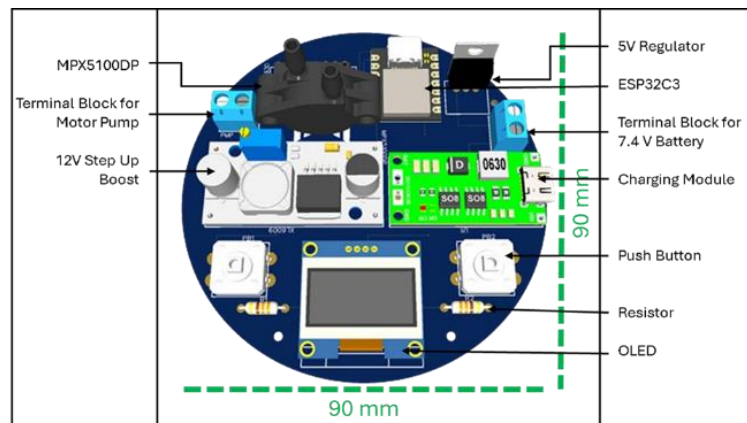


Figure 5. Optimized PCB layout of the portable cupping suction device

2.3. Software development

Software development focused on implementing control logic for the cupping modes and monitoring system states based on sensor feedbacks and user inputs. The system's flowchart, as shown in Figure 6, outlines the control logic and illustrates the sequential operations for mode selection, suction control, and sensor feedback evaluation. The system responded dynamically to user inputs, while successively maintaining pressure within the desired threshold.

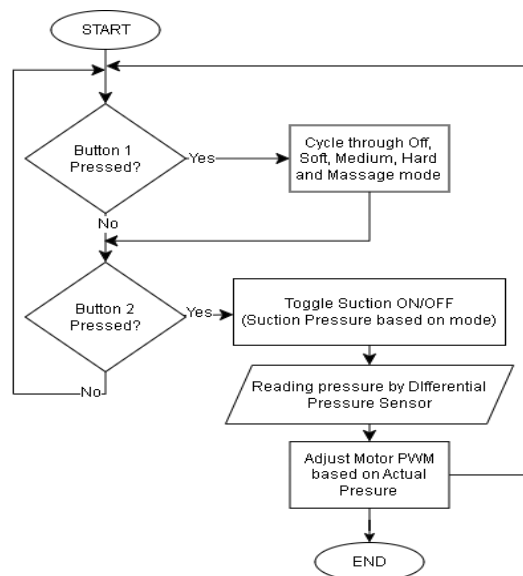


Figure 6. Flowchart illustrating system operation

2.4. Pre-experiment setup

Prior to conducting the experimental trials, a pre-experiment setup was established to ensure measurement accuracy and reliable controller performance. The differential pressure sensor was hereby calibrated for precise suction pressure measurement during the cupping process. Following this, parameters of the PID controller were configured based on the procedures of system identification.

Sensor calibration was performed to establish a linear relationship between outputs of the differential pressure sensor and values of the actual pressure. Additionally, system identification experiments were conducted to characterize the plant dynamics. The resulting plant model was used to determine the appropriate initial PID controller parameters for effective closed-loop regulation throughout subsequent testing.

2.4.1. Differential pressure sensor calibration

Accurate measurement of the negative pressure as generated by the motor pump is crucial for reliable operation of the portable cupping device. Therefore, a calibration procedure was conducted for the MPX5100DP differential pressure sensor to ensure measurement precision. This calibration process was systematically performed, and the steps are outlined as follows:

- a. Preparation and setup: All necessary components were prepared and assembled with accordance to the schematic as illustrated in Figure 7.

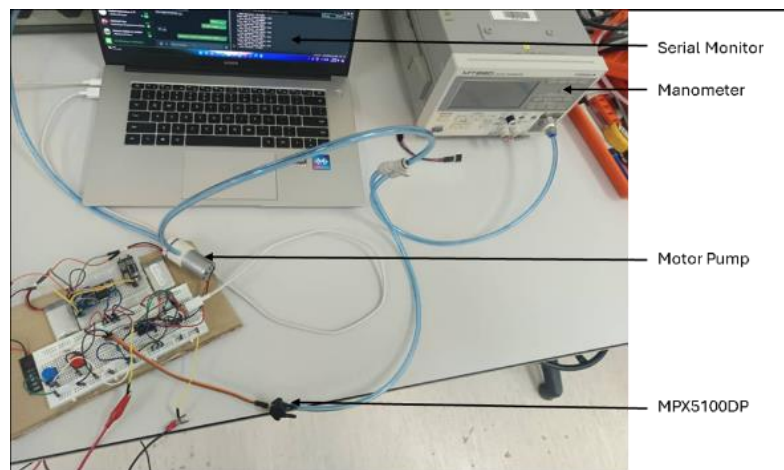


Figure 7. Setup for differential pressure sensor calibration

- b. Connection of components: The motor pump, manometer, pressure sensor, and a cupping cup were interconnected using flexible hose tubing with appropriate hose connectors to ensure airtight sealing.
- c. Programming the microcontroller: The ESP32C3 microcontroller was programmed to: i) Generate a PWM signal which controls the motor pump speed on a range between 0 and 255, ii) Acquire real-time digital output from the MPX5100DP sensor, and iii) Display the sensor readings through the serial monitor interface.
- d. Data acquisition: At each PWM increment, simultaneous readings from both the manometer and the pressure sensor were recorded and tabulated. The collected data is presented in Table 1.

Table 1. Calibration data for the MPX5100DP sensor

Motor PWM	Sensor digital value	Manometer reading (kPa)
40	747	-4.00
60	1246	-10.60
80	1994	-23.00
100	3900	-57.40
120	4095	-59.40

- e. Data analysis: A calibration curve was generated by plotting the sensor's digital outputs against the corresponding manometer readings, as shown in Figure 8. Resulting graph demonstrates a strong linear relation-

ship between the sensor outputs and the actual pressure values. Accordingly, best-fit line for the calibration data is given by the equation:

$$y = -0.01689x + 9.50348 \quad (1)$$

where y represents the pressure in kilopascals (kPa) and x denotes the sensor's digital value. This linear equation allows accurate conversion of sensor readings into real pressure values, which is critical in ensuring the precision of subsequent experimental measurements.

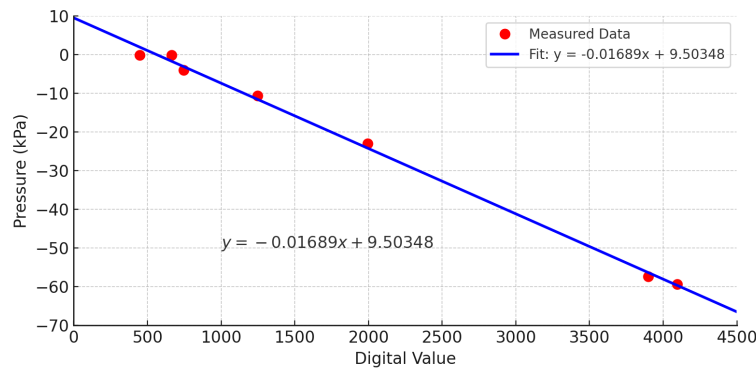


Figure 8. Calibration curve: Pressure sensor digital output versus manometer readings

2.4.2. PID regulation setting

To maintain the desired negative pressure within the cupping suction system, a PID control scheme was implemented. Proper tuning of the PID parameters is critical to ensure precise and stable pressure regulation. Two complementary strategies were sequentially employed for tuning, starting with system identification to derive an accurate system model, followed by PID controller optimization based on the identified model. Figure 9 illustrates the block diagram of the closed-loop PID control system as implemented for the portable cupping device.

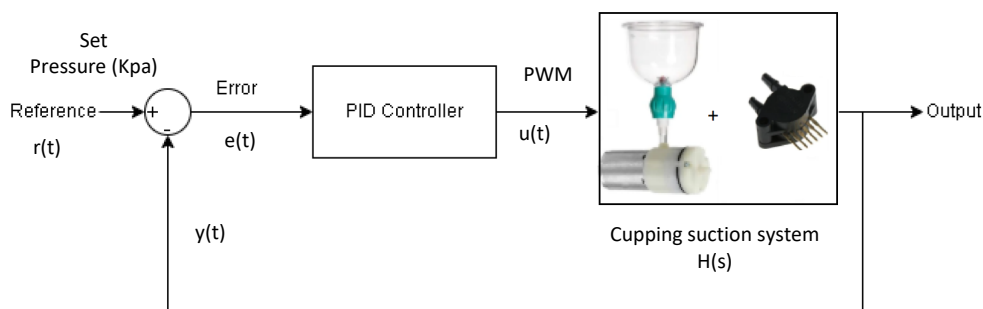


Figure 9. Block diagram of the closed-loop PID control system for the cupping suction device

- a. System identification: To establish a model of the cupping suction dynamics, PWM signals with varying duty cycles were applied to the motor pump. Suction pressure readings were recorded every 10 seconds over a 160-second window. The acquired time-series data were imported into MATLAB's system identification Toolbox, where a second-order transfer function was estimated using the estimation tool. The resulting transfer function is identified as (2):

$$H(s) = -\frac{0.008579}{s^2 + 0.9434s + 0.0209} \quad (2)$$

Achieving a fitting accuracy of approximately 70%, the identified model is deemed sufficient for controller design purposes. It is important to note that the data acquisition was conducted on a clean, instead of hairy, skin surface to ensure the validity of identified linear model.

- b. PID controller tuning: Achieving precise pressure regulation further propagated the development and simulation of a closed-loop system in Simulink based on the identified plant transfer function as presented in Equation (2). The plant dynamics in the Laplace domain are characterized by (3):

$$H(s) = \frac{Y(s)}{U(s)} \quad (3)$$

where $Y(s)$ and $U(s)$ denote the Laplace transforms of the system output $y(t)$ and the control input $u(t)$, respectively. They are separately defined as (4), (5):

$$Y(s) = \mathcal{L}\{y(t)\} = \int_0^{\infty} y(t)e^{-st} dt \quad (4)$$

$$U(s) = \mathcal{L}\{u(t)\} = \int_0^{\infty} u(t)e^{-st} dt \quad (5)$$

A PID controller was incorporated into the closed-loop model to regulate the system output. The control law of this controller in the time domain is expressed as (6):

$$u(t) = K_p e(t) + K_i \int e(t) dt + K_d \frac{de(t)}{dt} \quad (6)$$

where $e(t) = r(t) - y(t)$ is the tracking error between reference input $r(t)$ and measured output $y(t)$, with K_p , K_i , and K_d respectively represent the proportional, integral, and derivative gains.

Initial PID tuning was performed using Simulink's auto-tuning feature to establish the baseline gain values. Further refinement was conducted using MATLAB's PID Tuner, with optimization criteria focusing on the minimization of overshoot, the reduction of settling time, and the achievement of negligible steady-state error. Ultimately, the finalized optimized PID parameters are:

$$K_p = -4, \quad K_i = -0.17, \quad K_d = 4.45 \quad (7)$$

These parameters were subsequently implemented in the embedded controller of the portable cupping device to regulate negative pressure during real-time operation. Figure 9 illustrates the overall closed-loop system architecture, where $r(t)$ represents the reference input and $y(t)$ denotes the system's output.

2.5. Experimental procedures for cupping methods

Three distinct cupping techniques—massage cupping, dry cupping, and wet cupping—were evaluated for performance appraisal of the developed device. Table 2 summarizes the procedural steps, application duration, targeted body areas, and skin types for each cupping method.

Table 2. Experimental procedures and parameters for different cupping methods

Cupping method	Procedural steps	Time (s)	Body area	Skin type
Massage cupping	The targeted area is cleaned with an alcohol swab prior applying a small amount of oil for lubrication. The cup is placed and vacuum suction is initiated. The cup is then glided along a predefined path to perform the massage technique.	100	Back	Clean skin surface
Dry cupping	The treatment area is sanitized with an alcohol swab. A cup is placed on the skin and vacuum suction is applied to maintain negative pressure without subsequent movement.	60	Back, calves	Clean or slightly hairy skin
Wet cupping	The skin is disinfected and initial suction is applied. The cup is removed after several minutes with the area being incised superficially before reapplication of suction to facilitate blood extraction.	60	Back	Clean skin surface

3. EXPERIMENTAL SETUP AND RESULTS

Figure 10 presents the final prototype of the portable cupping suction device. Its upper compartment houses the PCB, battery, OLED display (visible through a designated opening), and control buttons for mode selection and motor operation. Its lower compartment contains the motor pump connected via flexible hoses to the differential pressure sensor and the cupping head held securely by a dedicated holder. A series of experiments were conducted to evaluate the device's suction accuracy, pressure control performance, and operational reliability across different cupping techniques and skin types. Dry and wet cupping sessions were performed at the targeted pressures of -25 kPa, -35 kPa, and -45 kPa for dry cupping, and -45 kPa for wet cupping. Massage cupping was conducted for 100 seconds at -25 kPa, with adjustments made via a wireless web server interface. System performance was then assessed across the procedures through the use of PID response graphs.

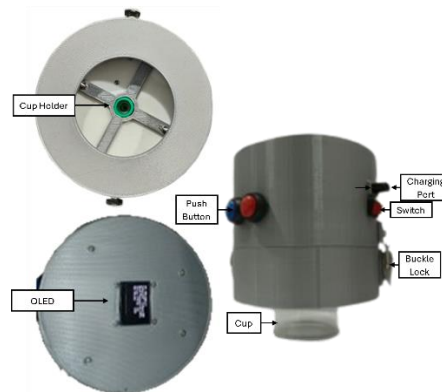


Figure 10. Final setup of the portable cupping suction device

3.1. Massage cupping

The massage cupping experiment focused on evaluating pressure regulation accuracy and dynamic PID control performance during active cup movement. The pressure was initially set at -15 kPa, followed by later adjustment at -25 kPa for enhanced skin adherence and massage efficacy. The procedure followed the steps outlined in Table 2. The cup was moved along a predefined trajectory on the back, as illustrated in Figure 11.



Figure 11. Massage cupping path on the back surface

Performance of PID control for the massage cupping session is illustrated in Figure 12. The actual pressure (blue curve) initially exhibited a significant overshoot before settling toward the desired setpoint (black dashed line). Over time, the closed-loop system demonstrated good tracking accuracy, with the real pressure fluctuating within acceptable bounds around the target value. The minimal steady-state error as observed during steady-state operation correspondingly indicates effective tuning of the PID controller for dynamic massage conditions. Quantitative evaluation of tracking performance was conducted by calculating the mean square error (MSE) and normalized error with respect to the setpoint. As summarized in Table 3, the system achieved a relatively low MSE of 10.9564 kPa^2 and a normalized error of 13.24% to indicate an overall satisfactory pressure regulation.

Importantly, the observed pressure response is considered acceptable for massage cupping applications. Despite the initial transient, the system consistently maintained a negative pressure level that ensures

secured cup attachment on the skin throughout the session. Furthermore, the pressure variations remained within the clinically acceptable limits which avoid excessive suction that can cause discomfort or injury. This stable and controlled pressure environment is essential toward achieving effective massage benefits, while ensuring safety and comfort of the patient.

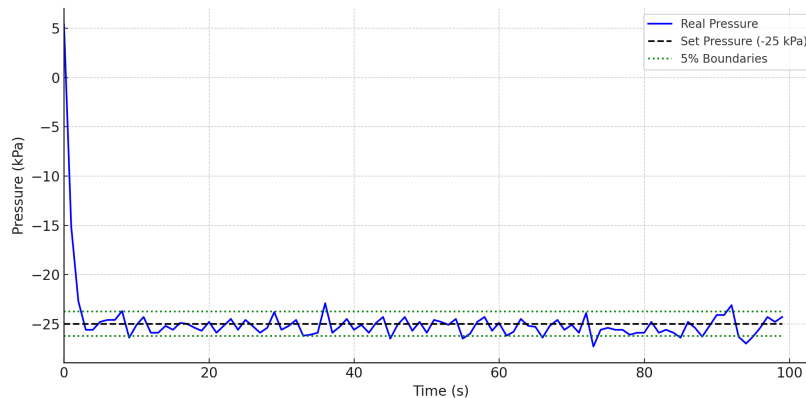


Figure 12. PID response during massage cupping

Table 3. Error metrics of PID control during massage cupping based on pressure tracking performance

Metric	Value
Mean square error (MSE) (kPa^2)	10.9564
Normalized error (%)	13.24%

3.2. Dry cupping

Dry cupping experiments were conducted under three system modes—soft, medium, and hard—applied to different skin types: clean (back), less hairy (calf), and slightly hairy (calf). The targeted suction pressures were -25 kPa, -35 kPa, and -45 kPa, respectively.

3.2.1. Soft mode on clean skin

In soft mode (-25 kPa), the device was tested on clean back skin. This mode is typically used in dry cupping applications aimed at relaxation therapy, as well as individuals with sensitive skin, where mild suction would sufficiently stimulate circulation without causing discomfort. As shown in Figure 13, a securely attached suction cup with minimal discomfort during the cupping session indicates good user tolerance and effective pressure engagement.



Figure 13. Soft mode application on clean back surface

The corresponding PID responses are presented in Figure 14. The system achieved a rapid drop in pressure toward the targeted setpoint with minimal fluctuation and no excessive overshoot. These characteristics indicate a stable and smooth response which suits sensitive skin. The gathered quantitative error metrics including the mean square error (MSE) and normalized error are further summarized in Table 4.

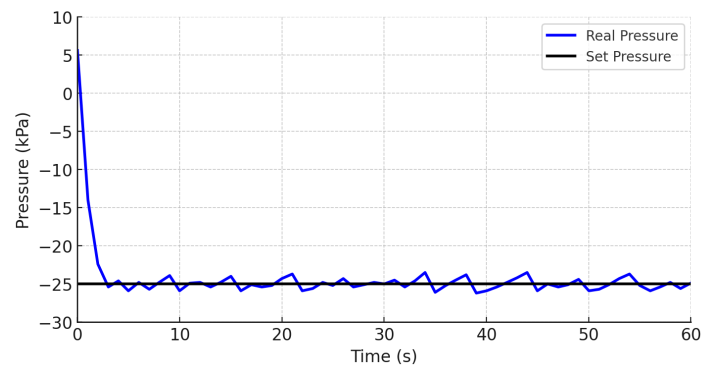


Figure 14. PID response for soft mode on clean skin

Table 4. Error metrics of PID response for soft mode on clean skin

Metric	Value
Mean square error (MSE) (kPa^2)	17.8949
Normalized error (%)	16.92%

3.2.2. Medium mode on less hairy skin

Following this, medium mode (-35 kPa) was tested on less hairy calf skin. This mode is typically utilized in dry cupping protocols that require moderate suction to stimulate deeper tissue layers, while preserving the patient's comfort. It is commonly applied to muscular regions such as the calf, thigh, or lower back, where enhanced circulation, myofascial release, and therapeutic decompression are desired. Herewith, initial suction attachment during the procedure is depicted in Figure 15.



Figure 15. Medium mode application on less hairy calf surface

The PID responses corresponding to this configuration are presented in Figure 16. Tested system exhibited an initial overshoot which approximately reaches a pressure of -40 kPa , followed by damped oscillations that progressively stabilized around the targeted setpoint. Stabilization was achieved nearing the periodical mark of 30 seconds to demonstrate the controller's effective accommodation for varying skin compliance and dynamic tissue behavior. Despite the initial transient response, the pressure was maintained within an acceptable therapeutic range for effective cupping without inducing discomfort of the patient.

Quantitative evaluations of the control performance are summarized in Table 5. Observably, the measured mean square error (MSE) and normalized tracking error are correspondingly recorded at 43.7672 kPa^2 and 18.90%. Nevertheless, the marginally higher values as compared to soft mode applications fall within the acceptable operational limits of medium-intensity cupping where greater pressure depth is targeted. Such results confirm the effectiveness of PID controller on robust and reliable pressure regulation for medium dry cupping sessions.

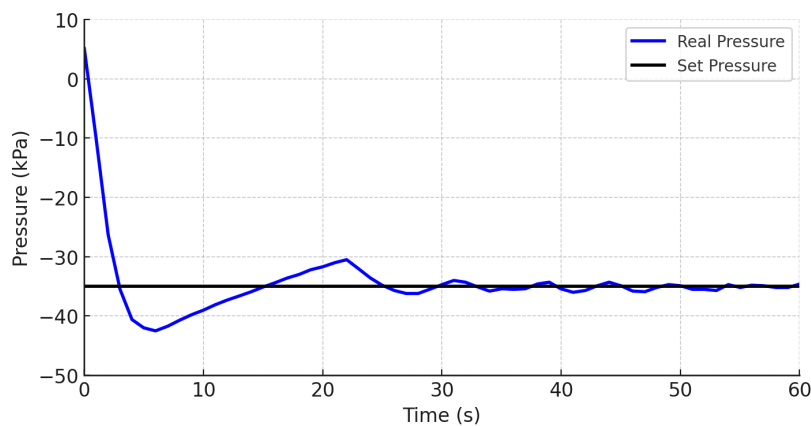


Figure 16. PID response for medium mode on less hairy skin

Table 5. Error metrics of PID response for medium mode on less hairy skin

Metric	Value
Mean square error (MSE) (kPa^2)	43.7672
Normalized error (%)	18.90%

3.2.3. Hard mode on slightly hairy skin

Hard mode (-45 kPa) was subsequently applied to slightly hairy calf skin. This mode is typically employed in therapeutic dry cupping applications that require deeper negative pressure level to achieve stronger tissue decompression and enhanced microcirculation. Figure 17 illustrates attachment of the suction cup on the targeted surface.

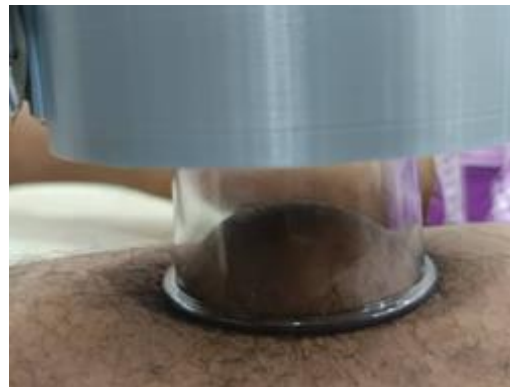


Figure 17. Hard mode application on slightly hairy skin

The corresponding PID responses are presented in Figure 18. Initial pressure fluctuations are observed during the first 25 seconds of the session, primarily caused by minor air leakage and uneven contact associated with hair interference on the skin surface. Nevertheless, the controller effectively stabilized the pressure toward the desired setpoint in demonstrating strong disturbance rejection capability and robust control performance under challenging adhesion conditions. Following the transient phase, the system maintained a steady negative pressure to ensure a continuously secured cup attachment without inducing excessive suction that can compromise comfort or safety.

Quantitative analysis of the tracking performance is summarized in Table 6. The mean square error (MSE) was calculated to be 64.9259 kPa^2 at the normalized tracking error of 17.91%. The relatively higher MSE against both soft and medium mode applications are justifiable within the clinically acceptable thresholds for hard cupping procedures. While the slightly elevated normalized error reflects an inherent difficulty

for continuous maintaining of perfect sealing on hairy surfaces, ultimate achievement of stabilized pressure indicates the system's adequacy in ensuring therapeutic efficacy without significant patient discomfort.

The higher negative pressure applied during hard mode, however, comes with a notable precaution of limiting each treatment session to a maximum of five minutes to minimize the risk of skin blistering, bruising, or other adverse effects. Adhering to appropriate time limit would, therefore, ensure both treatment safety and optimal therapeutic outcomes.

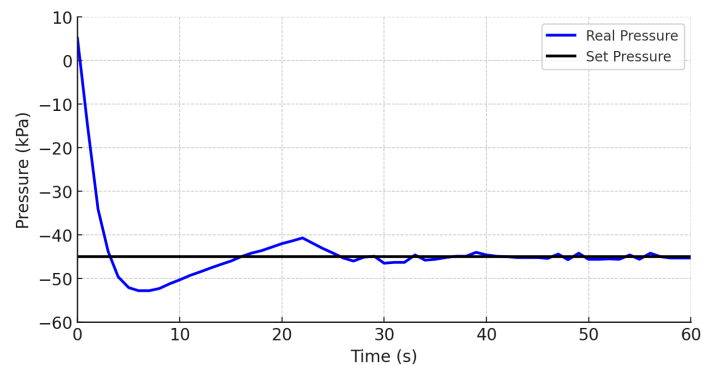


Figure 18. PID response for hard mode on slightly hairy skin

Table 6. Error metrics of PID response for hard mode on slightly hairy skin

Metric	Value
Mean square error (MSE) (kPa^2)	64.9259
Normalized error (%)	17.91%

3.3. Wet cupping

Procedure for wet cupping was conducted to evaluate the system's performance under more complex conditions of skin incisions and fluid collection within the cup. Unlike dry cupping which relies solely on negative pressure to stimulate tissues and enhance circulation, wet cupping additionally incorporates controlled superficial incisions to facilitate the extraction of stagnant blood and interstitial fluid. Such dual mechanism demands more precise pressure regulation to prevent excessive bleeding, discomfort, and the loss of vacuum integrity.

The current experiment especially applied medium mode suction (-35 kPa) on a clean back surface. Began with an initial warm-up phase using dry cupping, the procedure followed with skin sterilization using an alcohol swab. The suction cup was reapplied after making shallow and sterile incisions on the affected area with the reinstating of negative pressure to initiate fluid extraction. The result is illustrated in Figure 19.



Figure 19. Wet cupping procedure using medium mode

Generated responses for PID pressure control during the wet cupping session are presented in Figure 20. The system demonstrated rapid convergence toward the target setpoint, with minor fluctuations as attributed to progressive fluid accumulation within the cup. While fluid accumulation can momentarily disturb the vacuum seal and alter the internal pressure dynamics, the controller would promptly compensate such disturbances. Overall, the system maintained a stable and effective negative pressure throughout the treatment by ensuring safe and continuous fluid extraction without losing the adhesion.

Quantitative analysis of the control performance is summarized in Table 7, where the mean square error (MSE) was found to be 33.7790 kPa^2 with a normalized tracking error of 16.61%. Inherently more dynamic than the dry cupping sessions, these values indicate acceptable control performance under the wet cupping conditions. As shown, relatively modest increase in error highlights the controller's robustness and adaptability in managing pressure fluctuations brought about by fluid dynamics. Thus, the system remains suitable for clinical wet cupping applications where stable negative pressure is critical for both therapeutic efficacy and the patient's safety.

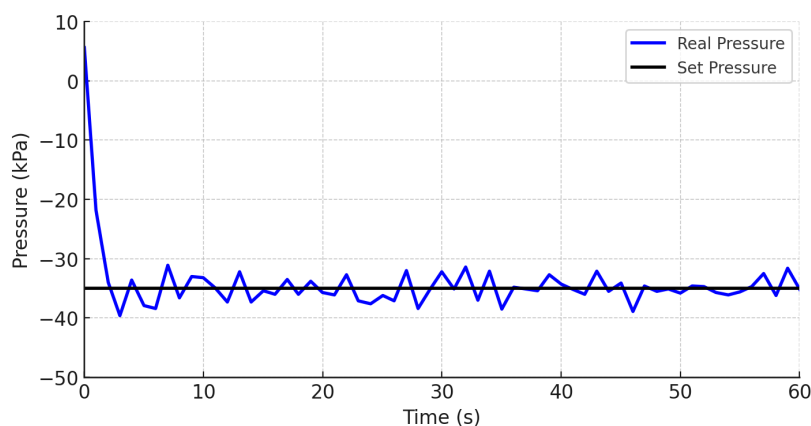


Figure 20. PID response during wet cupping

Table 7. Error metrics of PID response during wet cupping

Metric	Value
Mean square error (MSE) (kPa^2)	33.7790
Normalized error (%)	16.61%

4. CONCLUSION

The developed portable cupping suction device successfully achieved robust and accurate pressure regulation across various cupping modalities and skin conditions. Experimental results validated the system's ability to maintain stable negative pressure through PID control under different scenarios. Generated findings reveal rapid stabilization with minimal steady-state error was achieved in message cupping, consistent suction was maintained across clean, less hairy, and slightly hairy skin surfaces in dry cupping, as well as the effective management of pressure fluctuations as resulted from fluid accumulation in wet cupping to ensure firm, stable, and persisting suction. Quantitative evaluations, including mean square error and normalized error analysis, further affirmed the system's reliable tracking performance under dynamic conditions.

Empirically, the proposed and developed device demonstrated strong potential for clinical and therapeutic cupping applications. Such outcomes, thus, set the future trajectory for an improved long-term durability, the incorporation of wireless monitoring, and an expansion in clinical validation.

ACKNOWLEDGMENTS

The authors would like to express their in-depth gratitude to Universiti Malaysia Pahang Al-Sultan Abdullah (UMPSA) the research facilities and required supports as provided for this project.

FUNDING INFORMATION

This research was funded by Universiti Malaysia Pahang Al-Sultan Abdullah (UMPSA) under the RDU Grant (Reference: RDU240324).

AUTHOR CONTRIBUTIONS STATEMENT

This journal uses the Contributor Roles Taxonomy (CRediT) to recognize individual author contributions, reduce authorship disputes, and facilitate collaboration.

Name of Author	C	M	So	Va	Fo	I	R	D	O	E	Vi	Su	P	Fu
Mohd Riduwan bin Ghazali	✓	✓		✓	✓		✓	✓	✓	✓	✓	✓	✓	✓
Mohd Ashraf bin Ahmad	✓	✓	✓	✓	✓	✓	✓	✓	✓	✓	✓		✓	
Lugman Hakim Bin Akmalmas	✓		✓	✓		✓	✓		✓		✓		✓	

C	: Conceptualization	I	: Investigation	Vi	: Visualization
M	: Methodology	R	: Resources	Su	: Supervision
So	: Software	D	: Data Curation	P	: Project Administration
Va	: Validation	O	: Writing - Original Draft	Fu	: Funding Acquisition
Fo	: Formal Analysis	E	: Writing - Review & Editing		

REFERENCES

[1] K. Abbshar and H. Ahmed, "Effects of wet cupping (al-hijamah) on cholesterol in a sudanese population," *Journal of Acupuncture Research*, vol. 40, no. 4, pp. 351-355, 2023, doi: 10.13045/jar.2023.00213.

[2] S. Vanadia and N. Hidayati, "Cupping therapy's role in pain management: A literature review," *International Journal of Scientific Advances*, vol. 4, no. 2, pp. 101-108, 2022, doi: 10.51542/ijscia.v3i2.20.

[3] A. A Mohamed, X. Zhang, and Y. K Jan, "Evidence-based and adverse-effects analyses of cupping therapy in musculoskeletal and sports rehabilitation: A systematic and evidence-based review," *Journal of Back and Musculoskeletal Rehabilitation*, vol. 36, no. 1, pp. 3-19, 2023, doi: 10.3233/BMR-210242.

[4] J. Mirza, Y. Obaid, and I. Naseem, "Cupping therapy: A prudent approach in pain management—a systematic review," *Pakistan Journal of Rehabilitation*, vol. 10, no. 1, pp. 1-6, 2021, doi: 10.36283/pjr.zu.10.1/003.

[5] Y. Kim, Y. Oh, J. Kim, E. Kim, G. Y. Yang, and B. R. Lee, "The risk of applying moving cupping therapy to a patient with chronic lumbar pain previously treated with gold thread therapy," *Journal of Acupuncture Research*, pp. 317-322, 2022, doi: 10.13045/jar.2022.00192.

[6] A. M. Al-Bedah, I. S. Elsubai, N. A. Qureshi, T. S. Aboushanab, G. I. Ali, A. T. El-Olemy, ... M. S. Alqaed, "The medical perspective of cupping therapy: Effects and mechanisms of action," *Journal of Traditional and Complementary Medicine*, vol. 9, no. 2, pp. 125-130, 2019, doi: 10.1016/j.jtcme.2018.03.003.

[7] H. Tian, S. Wang, M. Fu, D. Ning, and Y. Gong, "Smart cup for in-situ 3d measurement of wall-mounted debris via 2d sensing grid," *Micromachines*, vol. 14, p. 489, 2023, doi: 10.3390/mi14020489.

[8] Y. Hamzehnejadi, P. M. Shahrababaki, M. Alnaiem, S. Mokhtarabad, H. Tajadini, A. Rashidinejad, J. Abbas, and M. Dehghan, "The impact of massage and dry cupping on dysrhythmia in cardiac patients: A randomized parallel controlled trial," *Journal of Bodywork and Movement Therapies*, vol. 38, pp. 417-424, 2024, doi: 10.1016/j.jbmt.2024.01.028.

[9] X. Qi, Y. Wang, and Z. Liu, "Influence of cupping therapy on skin lesion symptoms: A systematic review," *Journal of Traditional Chinese Medicine*, vol. 41, no. 3, pp. 301-307, 2021.

[10] X. Qiao, C. Yang, W. Yang, and Y. Li, "Moving cupping therapy combined with acupoint bloodletting for plaque psoriasis: A case report," *Explore*, vol. 21, no. 1, p. 103098, 2025, doi: 10.1016/j.explore.2024.103098.

[11] T. Yue, W. Si, A. Keller, C. Yang, H. Bloomfield-Gadêlha, and J. Rossiter, "Bioinspired multiscale adaptive suction on complex dry surfaces enhanced by regulated water secretion," in *Proceedings of the National Academy of Sciences*, vol. 121, no. 16, 2024, doi: 10.1073/pnas.2314359121.

[12] A. Elshanshory, S. Ahmed, and M. Ali, "Al-hijamah: An overview of the therapeutic effects and mechanism of action," *Journal of Traditional and Complementary Medicine*, vol. 8, no. 4, pp. 497-503, 2018.

[13] M. Alam and K. Abbas, "The role of cupping therapy (CT) in pain tackling, an insight into mechanism therapeutic effects and its relevance in current medical scenario," *International Journal of Current Science Research and Review*, vol. 4, no. 7, pp. 732-739, 2021, doi: 10.47191/ijcsrr/V4-i7-16.

[14] L. Chen, "Cupping therapy," in *Acupuncture Techniques: A Practical Manual*. Springer, 2024, pp. 143-163, doi: 10.1007/978-3-031-59272-0-10.




[15] H. Hidayat, M. Amiruddin, A. Fadilia Aktifa, M. C.Haryadi, and Nabila Azzahra, "Cupping therapy (Hijamah) in islamic and medical perspective," (in Bahasa) in *Proceedings of International Pharmacy Ulul Albab Conference and Seminar (PLANAR)*, Malang, August 10, 2022, doi: 10.18860/planar.v2i0.2129.

[16] M. N. A. M. Hayee, L. H. A. Shah, M. A. Hamidi, M. Z. Sulaiman, Z. Ahmad, R. Muda, and K. H. Ghazali, "Vacuum pressure comparison of cupping therapy device using multiple cups for cupping therapy improvements," in *AIP Conference Proceedings*, vol. 2998, no. 1, 2024, doi: 10.1063/5.0188774.




- [17] J. Kenny, A. Smith, and R. Johnson, "Effects of cupping therapy on pain management in patients with chronic back pain: A randomized controlled trial," *Journal of Alternative and Complementary Medicine*, vol. 29, no. 1, pp. 12–18, 2023.
- [18] J. Lee, G. W. Hwang, B. S. Lee, N. J. Park, S. N. Kim, D. Lim and C. Pang, "Artificial octopus-limb-like adhesive patches for cupping-driven transdermal delivery with nanoscale control of stratum corneum," *ACS Nano*, vol. 18, no. 7, pp. 5311–5321, 2024, doi: 10.1021/acsnano.3c09304.
- [19] C. Zhang, L. Liu, K. Xu, Z. Dong, Y. Ding, Q. Li, and P. Li, "Hydraulically coupled dielectric elastomer actuators for a bioinspired suction cup," *Polymers*, vol. 13, no. 20, p. 3481, 2024, doi: 10.3390/polym13203481.
- [20] R. Seredyński, T. Okupnik, P. Musz, S. Tubek, B. Ponikowska, and B. Paleczny, "Neck chamber technique revisited: Low-noise device delivering negative and positive pressure and enabling concomitant carotid artery imaging with ultrasonography," *Frontiers in Physiology*, vol. 12, 2021, doi: 10.3389/fphys.2021.703692.
- [21] M. R. Ghazali, M. A. Ahmad, Y. T. Hui, N. A. N. Shamsudin, and W. I. Ibrahim, "Cupping suction system with fuzzy logic controller design," in *2022 IEEE 10th Conference on Systems, Process Control (ICSPC)*. 2022, pp. 23–28, doi: 10.1109/IC-SPC55597.2022.10001794.
- [22] C. Gao, M. Wang, L. He, Y. He, and T. Li, "Alternations of hemodynamic parameters during chinese cupping therapy assessed by an embedded near-infrared spectroscopy monitor," *Biomedical Optics Express*, vol. 10, no. 1, pp. 196–205, 2018, doi: 10.1364/BOE.10.000196.
- [23] Y. Cui and Q. Zhang, "Review on advances in cupping therapy: Mechanisms, efficacy, and technology," *Frontiers in Medicine*, vol. 10, 2023.
- [24] A. T. Ajiboye, J. F. Opadiji, O. J. Popoola, and O. F. Adebayo, "Selection of pid controller design plane for time-delay systems using genetic algorithm," *International Journal of Electrical and Computer Engineering Systems*, vol. 13, no. 10, pp. 917–926, 2022, doi: 10.32985/ijeces.13.10.7.
- [25] Z. Li, "Review of pid control design and tuning methods," in *Journal of Physics: Conference Series*, vol. 2649, no. 1, p. 012009, 2023, doi: 10.1088/1742-6596/2649/1/012009.
- [26] B. Chi, H. Lee, and S. Park, "Effectiveness of cupping therapy for pain management: A systematic review and meta-analysis," *Pain Medicine*, vol. 17, no. 8, pp. 1491–1503, 2016.
- [27] J. Hu, Y. Zhao, and T. Wang, "Optimal protocols for cupping therapy in treating musculoskeletal disorders: A randomized controlled trial," *Journal of Traditional Chinese Medicine*, vol. 44, no. 2, pp. 123–130, 2024.

BIOGRAPHIES OF AUTHORS






Mohd Riduwan Ghazali    received the Ph.D. degree in electronics engineering from Universiti Malaysia Pahang (UMP) in 2020. He is currently a senior lecturer at the Faculty of Electrical and Electronics Engineering Technology, Universiti Malaysia Pahang Al-Sultan Abdullah (UMPSA). His research interests include data-driven control, control and instrumentation system design, mechatronics, robotics systems, and cupping system applications. He has led and contributed to various national research grants, publications in indexed journals, and community innovation projects. He can be contacted at email: riduwan@umpsa.edu.my.



Mohd Ashraf Ahmad    received his first degree in B.Eng. electrical mechatronics and master degree in M.Eng mechatronics and automatic control from University of Technology Malaysia (UTM) in 2006 and 2008, respectively. He received a Ph.D in Informatics (Systems Science) from Kyoto University in 2015. He is currently an associate professor in the Faculty of Electrical and Electronics Engineering Technology, University Malaysia Pahang Al-Sultan Abdullah (UMPSA). His current research interests are model-free control, control of mechatronic systems, nonlinear system identification and vibration control. He has been serving as an associate editor for the International Journal of Electrical and Computer Engineering since 2016, Applications of Modelling and Simulation since 2017, and Journal of Future Robot Life since 2019. He has been listed as the 2% of Stanford University's world's top scientists in 2022, 2023 and 2024. He can be contacted at email: mashraf@umpsa.edu.my.



Luqman Hakim Akmalmas    is currently pursuing his bachelor's degree at the Faculty of Electrical and Electronic Engineering Technology, Universiti Malaysia Pahang Al-Sultan Abdullah (UMPSA). His interests include hardware design, embedded systems, and mechatronic system development. He has participated in various student research projects focusing on smart healthcare devices. He can be contacted at email: luqman18700@gmail.com.